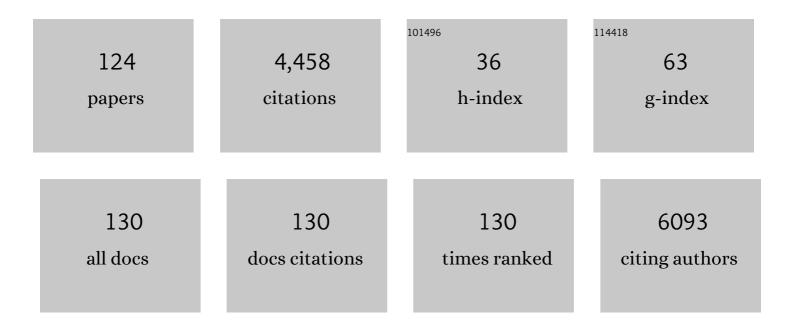
List of Publications by Year in descending order

Source: https://exaly.com/author-pdf/6088645/publications.pdf Version: 2024-02-01



#	Article	IF	CITATIONS
1	Large-Scale Synthesis of SnO ₂ Nanosheets with High Lithium Storage Capacity. Journal of the American Chemical Society, 2010, 132, 46-47.	6.6	626
2	Grain size dependent grain boundary defect structure: case of doped zirconia. Acta Materialia, 2003, 51, 2539-2547.	3.8	170
3	Evolution of the ωo phase in a β-stabilized multi-phase TiAl alloy and its effect on hardness. Acta Materialia, 2014, 64, 241-252.	3.8	144
4	Stability of Carbon Nanotubes: How Small Can They Be?. Physical Review Letters, 2000, 85, 3249-3252.	2.9	142
5	A simple method to synthesise single-crystalline manganese oxide nanowires. Chemical Physics Letters, 2003, 378, 349-353.	1.2	133
6	Structural Characteristics of Cerium Oxide Nanocrystals Prepared by the Microemulsion Method. Chemistry of Materials, 2001, 13, 4192-4197.	3.2	116
7	Giant heterogeneous magnetostriction in Fe–Ga alloys: Effect of trace element doping. Acta Materialia, 2016, 109, 177-186.	3.8	112
8	Atomic and electronic characterization of thea[100]dislocation core inSrTiO3. Physical Review B, 2002, 66, .	1.1	108
9	Graphene-templated synthesis of palladium nanoplates as novel electrocatalyst for direct methanol fuel cell. Applied Surface Science, 2019, 466, 385-392.	3.1	106
10	Electrical and Structural Characterization of a Lowâ€Angle Tilt Grain Boundary in Ironâ€Doped Strontium Titanate. Journal of the American Ceramic Society, 2003, 86, 922-928.	1.9	103
11	Deformation mechanisms of a modified 316L austenitic steel subjected to high pressure torsion. Materials Science & Engineering A: Structural Materials: Properties, Microstructure and Processing, 2011, 528, 2776-2786.	2.6	95
12	Electronic and atomic structure of a dissociated dislocation inSrTiO3. Physical Review B, 2002, 66, .	1.1	93
13	Fracture toughness and structural evolution in the TiAlN system upon annealing. Scientific Reports, 2017, 7, 16476.	1.6	93
14	Origin of large plasticity and multiscale effects in iron-based metallic glasses. Nature Communications, 2018, 9, 1333.	5.8	89
15	Direct Atom-Resolved Imaging of Oxides and Their Grain Boundaries. Science, 2003, 302, 846-849.	6.0	88
16	Synthesis, Thermal Stability and Properties of ZnO ₂ Nanoparticles. Journal of Physical Chemistry C, 2009, 113, 1320-1324.	1.5	79
17	New insights on the formation of supersaturated solid solutions in the Cu–Cr system deformed by high-pressure torsion. Acta Materialia, 2014, 69, 301-313.	3.8	73
18	Toughness enhancement in TiN/WN superlattice thin films. Acta Materialia, 2019, 172, 18-29.	3.8	72

#	Article	IF	CITATIONS
19	Influence of interrupted quenching on artificial aging of Al–Mg–Si alloys. Acta Materialia, 2012, 60, 4496-4505.	3.8	71
20	Electrical resistance of low-angle tilt grain boundaries in acceptor-doped SrTiO3 as a function of misorientation angle. Journal of Applied Physics, 2005, 97, 053502.	1.1	63
21	An Epitaxial Ferroelectric Tunnel Junction on Silicon. Advanced Materials, 2014, 26, 7185-7189.	11.1	61
22	Structure and Chemical Transformation in Cerium Oxide Nanoparticles Coated by Surfactant Cetyltrimethylammonium Bromide (CTAB):Â An X-ray Absorption Spectroscopic Study. Journal of Physical Chemistry B, 2002, 106, 4569-4577.	1.2	53
23	Comparative studies of microstructure and impedance of small-angle symmetrical and asymmetrical grain boundaries in SrTiO3. Acta Materialia, 2005, 53, 5007-5015.	3.8	49
24	Advanced nanomechanics in the TEM: effects of thermal annealing on FIB prepared Cu samples. Philosophical Magazine, 2012, 92, 3269-3289.	0.7	48
25	Synthesis and characterization of antimony oxide nanoparticles. Journal of Materials Research, 2001, 16, 803-805.	1.2	46
26	Behaviour of TEM metal grids during in-situ heating experiments. Ultramicroscopy, 2009, 109, 766-774.	0.8	44
27	Microstructure of cobalt oxide doped sintered ceria solid solutions. Journal of Electroceramics, 2006, 16, 191-197.	0.8	42
28	Fracture toughness of Ti-Si-N thin films. International Journal of Refractory Metals and Hard Materials, 2018, 72, 78-82.	1.7	40
29	Novel synthesis of core-shell Au-Pt dendritic nanoparticles supported on carbon black for enhanced methanol electro-oxidation. Applied Surface Science, 2018, 433, 840-846.	3.1	39
30	Surface effects in the energy loss near edge structure of different cobalt oxides. Ultramicroscopy, 2007, 107, 598-603.	0.8	38
31	Highâ€Performance Smallâ€Amount Fe ₂ O ₃ â€Doped (K,Na)NbO ₃ â€Based Leadâ€Free Piezoceramics with Irregular Phase Evolution. Journal of the American Ceramic Society, 2016, 99, 2341-2346.	1.9	38
32	Filling of single-walled carbon nanotubes with silver. Journal of Materials Research, 2000, 15, 2658-2661.	1.2	37
33	HRTEM and EELS study of screw dislocation cores inSrTiO3. Physical Review B, 2004, 69, .	1.1	37
34	Microstructure characterization of a cobalt-oxide-doped cerium-gadolinium-oxide by analytical and high-resolution TEM. Acta Materialia, 2007, 55, 2907-2917.	3.8	37
35	Lateral gradients of phases, residual stress and hardness in a laser heated Ti0.52Al0.48N coating on hard metal. Surface and Coatings Technology, 2012, 206, 4502-4510.	2.2	37
36	High electrocatalytic performance of a graphene-supported PtAu nanoalloy for methanolÂoxidation. International Journal of Hydrogen Energy, 2018, 43, 12803-12810.	3.8	37

#	Article	IF	CITATIONS
37	Oxygen-mediated deformation and grain refinement in Cu-Fe nanocrystalline alloys. Acta Materialia, 2019, 166, 281-293.	3.8	37
38	Insight into the structural evolution during TiN film growth via atomic resolution TEM. Journal of Alloys and Compounds, 2018, 754, 257-267.	2.8	36
39	On the stacking fault energy related deformation mechanism of nanocrystalline Cu and Cu alloys: A first-principles and TEM study. Journal of Alloys and Compounds, 2019, 776, 807-818.	2.8	36
40	Fracture properties of thin film TiN at elevated temperatures. Materials and Design, 2020, 194, 108885.	3.3	36
41	Grain boundary segregation in ultra-low carbon steel. Materials Science & Engineering A: Structural Materials: Properties, Microstructure and Processing, 2000, 291, 22-26.	2.6	35
42	Fracture toughness trends of modulus-matched TiN/(Cr,Al)N thin film superlattices. Acta Materialia, 2021, 202, 376-386.	3.8	35
43	Direct atomic identification of cation migration induced gradual cubic-to-hexagonal phase transition in Ge2Sb2Te5. Communications Chemistry, 2019, 2, .	2.0	32
44	Crystallographic orientation dependent maximum layer thickness of cubic AlN in CrN/AlN multilayers. Acta Materialia, 2019, 168, 190-202.	3.8	31
45	High-concentration nitrogen-doped carbon nanotube arrays. Nanotechnology, 2003, 14, 931-934.	1.3	30
46	Single-Phase Titania Nanocrystallites and Nanofibers from Titanium Tetrachloride in Acetone and Other Ketones. Inorganic Chemistry, 2007, 46, 5093-5099.	1.9	29
47	Correlating structural and mechanical properties of AlN/TiN superlattice films. Scripta Materialia, 2019, 165, 159-163.	2.6	29
48	Atomistic mechanisms underlying plasticity and crack growth in ceramics: a case study of AlN/TiN superlattices. Acta Materialia, 2022, 229, 117809.	3.8	29
49	Structural characterization of a Cu/MgO(001) interface using CS-corrected HRTEM. Thin Solid Films, 2010, 519, 1662-1667.	0.8	26
50	On the phase evolution and dissolution process in Cu-Cr alloys deformed by high pressure torsion. Scripta Materialia, 2017, 133, 41-44.	2.6	26
51	Magnetic properties and atomic structure of La2/3Ca1/3MnO3–YBa2Cu3O7 heterointerfaces. Applied Physics Letters, 2009, 95, .	1.5	25
52	Controllable synthesis of palladium nanocubes/reduced graphene oxide composites and their enhanced electrocatalytic performance. Journal of Power Sources, 2015, 280, 422-429.	4.0	25
53	Mechanical properties and epitaxial growth of TiN/AlN superlattices. Surface and Coatings Technology, 2019, 375, 1-7.	2.2	25
54	Correlating elemental distribution with mechanical properties of TiN/SiNx nanocomposite coatings. Scripta Materialia, 2019, 170, 20-23.	2.6	23

#	Article	IF	CITATIONS
55	Schottky barrier formed by network of screw dislocations in SrTiO3. Applied Physics Letters, 2005, 87, 162105.	1.5	22
56	Insights into the atomic and electronic structure triggered by ordered nitrogen vacancies in CrN. Physical Review B, 2013, 87, .	1.1	22
57	The peculiarity of the metal-ceramic interface. Scientific Reports, 2015, 5, 11460.	1.6	22
58	Pt nanoparticles modified Au dendritic nanostructures: Facile synthesis and enhanced electrocatalytic performance for methanol oxidation. International Journal of Hydrogen Energy, 2017, 42, 22100-22107.	3.8	22
59	Non-equilibrium intergranular segregation in ultra low carbon steel. Materials Science and Technology, 2000, 16, 305-308.	0.8	21
60	Electrical properties and structure of grain boundaries in n-conducting BaTiO3 ceramics. Journal of the European Ceramic Society, 2011, 31, 763-771.	2.8	21
61	Ultrafast Giant Photostriction of Epitaxial Strontium Iridate Film with Superior Endurance. Nano Letters, 2018, 18, 7742-7748.	4.5	21
62	Vanadium- and chromium-containing mesoporous MCM-41 molecular sieves with hierarchical structure. Microporous and Mesoporous Materials, 2001, 43, 227-236.	2.2	20
63	Anomalous compressive behavior in CeO ₂ nanocubes under high pressure. New Journal of Physics, 2008, 10, 123016.	1.2	19
64	Dislocation densities and alternating strain fields in CrN/AlN nanolayers. Thin Solid Films, 2017, 638, 189-200.	0.8	19
65	Atomic insights on intermixing of nanoscale nitride multilayer triggered by nanoindentation. Acta Materialia, 2021, 214, 117004.	3.8	19
66	Microstructural evolution and grain refinement in an intermetallic titanium aluminide alloy with a high molybdenum content. International Journal of Materials Research, 2015, 106, 725-731.	0.1	18
67	Correlating point defects with mechanical properties in nanocrystalline TiN thin films. Materials and Design, 2021, 207, 109844.	3.3	18
68	In-situ tracking the structural and chemical evolution of nanostructured CuCr alloys. Acta Materialia, 2017, 138, 42-51.	3.8	17
69	Microstructure characterization of Al–Cr–Fe quasicrystals sintered using spark plasma sintering. Materials Characterization, 2015, 110, 264-271.	1.9	16
70	Revealing the Microstructural evolution in Cu-Cr nanocrystalline alloys during high pressure torsion. Materials Science & Engineering A: Structural Materials: Properties, Microstructure and Processing, 2017, 695, 350-359.	2.6	16
71	Combined Fe and O effects on microstructural evolution and strengthening in Cu–Fe nanocrystalline alloys. Materials Science & Engineering A: Structural Materials: Properties, Microstructure and Processing, 2020, 772, 138800.	2.6	16
72	Structural imaging of Î ² -Si3N4 by spherical aberration-corrected high-resolution transmission electron microscopy. Ultramicroscopy, 2009, 109, 1114-1120.	0.8	15

#	Article	IF	CITATIONS
73	Influence of phase transformation on the damage tolerance of Ti-Al-N coatings. Vacuum, 2018, 155, 153-157.	1.6	15
74	The observation of Co film oxidation on Si and SiO2 substrates. Thin Solid Films, 1996, 286, 295-298.	0.8	14
75	In situ atomic-scale observation of oxidation and decomposition processes in nanocrystalline alloys. Nature Communications, 2018, 9, 946.	5.8	14
76	Superlattice-induced oscillations of interplanar distances and strain effects in the CrN/AlN system. Physical Review B, 2017, 95, .	1.1	13
77	Study of the double layer CeO2/Nb2O5 thin film. Journal of Vacuum Science and Technology A: Vacuum, Surfaces and Films, 2000, 18, 2928-2931.	0.9	12
78	Synthesis and Microstructure of Antimony Oxide Nanorods. Journal of Materials Research, 2002, 17, 1698-1701.	1.2	12
79	In Situ Study of γâ€TiAl Lamellae Formation in Supersaturated α ₂ â€Ti ₃ Al Grains. Advanced Engineering Materials, 2012, 14, 299-303.	1.6	12
80	On nanostructured molybdenum–copper composites produced by high-pressure torsion. Journal of Materials Science, 2017, 52, 9872-9883.	1.7	12
81	Morphogenesis of surface patterns and incorporation of redox-active metals in mesoporous silicate molecular sieves. Surface and Interface Analysis, 2001, 32, 193-197.	0.8	11
82	Thin tantalum–silicon–oxygen/tantalum–silicon–nitrogen films as high-efficiency humidity diffusion barriers for solar cell encapsulation. Thin Solid Films, 2006, 515, 1612-1617.	0.8	11
83	Homogeneity of the superplastic Zr _{64.13} Cu _{15.75} Ni _{10.12} Al ₁₀ bulk metallic glass. Journal of Materials Research, 2009, 24, 3116-3120.	1.2	11
84	Real-time atomic-resolution observation of coherent twin boundary migration in CrN. Acta Materialia, 2021, 208, 116732.	3.8	10
85	The formation of TiO ₂ /VO ₂ multilayer structure <i>via</i> directional cationic diffusion. Nanoscale, 2021, 13, 7783-7791.	2.8	10
86	Comprehensive characterization of iron oxide containing mesoporous molecular sieve MCM-41. Studies in Surface Science and Catalysis, 2002, , 403-410.	1.5	8
87	Growth-twins in CrN/AlN multilayers induced by hetero-phase interfaces. Acta Materialia, 2020, 185, 157-170.	3.8	8
88	Strain-induced structure and oxygen transport interactions in epitaxial La0.6Sr0.4CoO3â~δ thin films. Communications Materials, 2020, 1, .	2.9	8
89	Current Oscillations in the Layer-by-Layer Electrochemical Deposition of Vertically Aligned Nanosheets of Zinc Hydroxide Nitrate. Journal of the Electrochemical Society, 2013, 160, D558-D564.	1.3	7
90	Revealing the atomic and electronic structure of a SrTiO3/LaNiO3/SrTiO3 heterostructure interface. Journal of Applied Physics, 2014, 115, 103519.	1.1	7

#	Article	IF	CITATIONS
91	Indentation response of a superlattice thin film revealed by in-situ scanning X-ray nanodiffraction. Acta Materialia, 2020, 195, 425-432.	3.8	7
92	Atomic-scale study on incoherent twin boundary evolution in nanograined Cu. Scripta Materialia, 2020, 186, 278-281.	2.6	7
93	Nitrogen atom shift and the structural change in chromium nitride. Acta Materialia, 2015, 98, 119-127.	3.8	6
94	Microstructural and texture evolution of copper-(chromium, molybdenum, tungsten) composites deformed by high-pressure-torsion. International Journal of Refractory Metals and Hard Materials, 2018, 75, 137-146.	1.7	6
95	Mapping the mechanical properties in nitride coatings at the nanometer scale. Acta Materialia, 2020, 194, 343-353.	3.8	6
96	Atomic-scale understanding of the structural evolution of TiN/AlN superlattice during nanoindentation— Part 1: Deformation. Acta Materialia, 2022, 234, 118008.	3.8	6
97	Electron energy-loss spectroscopy study of a multilayered SiOx and SiOxCy film prepared by plasma-enhanced chemical vapor deposition. Journal of Materials Research, 2006, 21, 608-612.	1.2	5
98	Atomic and electronic structures of a transition layer at the CrN/Cr interface. Journal of Applied Physics, 2011, 110, 043524.	1.1	5
99	Orientation of FePt nanoparticles on top of a-SiO ₂ /Si(001), MgO(001) and sapphire(0001): effect of thermal treatments and influence of substrate and particle size. Beilstein Journal of Nanotechnology, 2016, 7, 591-604.	1.5	5
100	Complementary High Spatial Resolution Methods in Materials Science and Engineering. Advanced Engineering Materials, 2017, 19, 1600671.	1.6	5
101	Transmission electron microscopical study of teenage crown dentin on the nanometer scale. Materials Science and Engineering C, 2017, 71, 994-998.	3.8	5
102	Study on Ca Segregation toward an Epitaxial Interface between Bismuth Ferrite and Strontium Titanate. ACS Applied Materials & Interfaces, 2020, 12, 12264-12274.	4.0	5
103	The Route to Supercurrent Transparent Ferromagnetic Barriers in Superconducting Matrix. ACS Nano, 2019, 13, 5655-5661.	7.3	4
104	Atomic-scale investigation on the structural evolution and deformation behaviors of Cu–Cr nanocrystalline alloys processed by high-pressure torsion. Journal of Alloys and Compounds, 2020, 832, 154994.	2.8	4
105	Negatively Charged In-Plane and Out-Of-Plane Domain Walls with Oxygen-Vacancy Agglomerations in a Ca-Doped Bismuth-Ferrite Thin Film. ACS Applied Electronic Materials, 2021, 3, 4498-4508.	2.0	4
106	Irradiation-induced dissociation of ana⟠100⟩ edge dislocation in SrTiO3. Philosophical Magazine Letters, 2003, 83, 711-719.	0.5	3
107	Unveiling the atomic and electronic structure of the VN/MgO interface. Physical Review B, 2010, 82, .	1.1	3
108	Dynamic behavior of nanometer-scale amorphous intergranular film in silicon nitride by in situ high-resolution transmission electron microscopy. Journal of the European Ceramic Society, 2011, 31, 1835-1840.	2.8	3

#	Article	IF	CITATIONS
109	Transmission electron microscopy characterization of CrN films on MgO(001). Thin Solid Films, 2013, 545, 154-160.	0.8	3
110	Crossover between superconductivity and magnetism in SrRuO ₃ mesocrystal embedded YBa ₂ Cu ₃ O _{7â[°]x} heterostructures. Nanoscale, 2016, 8, 18454-18460.	2.8	3
111	Atomic resolution analyses on defects in nanocrystalline Cu-based alloys generated by severe plastic deformation. Materials Characterization, 2019, 157, 109886.	1.9	3
112	Atomic-scale understanding of the structural evolution in TiN/AlN superlattice during nanoindentation—Part 2: Strengthening. Acta Materialia, 2022, 234, 118009.	3.8	3
113	Growth of compound single- and multi-walled carbon nanotubes. Ultramicroscopy, 2004, 98, 195-200.	0.8	2
114	Interfacial microstructure and defect analysis in Cu(In,Ga)Se([sub]2)-based multilayered film by analytical transmission electron microscopy and focused ion beam. Thin Solid Films, 2009, 517, 4329-4335.	0.8	2
115	Uniformly distributed nickel nanoparticles created by heating the carbon nanotube. Journal of Materials Research, 2003, 18, 604-608.	1.2	1
116	Compound growth and microstructure of carbon nanotube. Journal of Materials Research, 2003, 18, 2459-2463.	1.2	1
117	<i>In Situ</i> TEM Heating Study of the γ Lamellae Formation inside the α ₂ Matrix of a Ti-45Al-7.5Nb Alloy. Advanced Materials Research, 0, 146-147, 1365-1368.	0.3	1
118	Local symmetry breaking of a thin crystal structure of Â-Si3N4 as revealed by spherical aberration corrected high-resolution transmission electron microscopy images. Journal of Electron Microscopy, 2012, 61, 145-57.	0.9	1
119	PLD growth and characteristics of lead-free NKLNST ferroelectric nanotubes. Journal of Materials Research and Technology, 2020, 9, 12818-12823.	2.6	1
120	Ca Solubility in a BiFeO ₃ -Based System with a Secondary Bi ₂ O ₃ Phase on a Nanoscale. Journal of Physical Chemistry C, 2022, 126, 7696-7703.	1.5	1
121	Characterization of the microstructure of Co thin film on silicon substrate by TEM. Journal of Electronic Materials, 2000, 29, 617-621.	1.0	0
122	Study on the Atomic and Electronic Structure in CrN (VN, TiN) Films using CS-Corrected TEM. Microscopy and Microanalysis, 2015, 21, 2079-2080.	0.2	0
123	Toughness Enhancement in TiN/WN Superlattice Thin Films. SSRN Electronic Journal, 0, , .	0.4	0
124	Tracking the Structural and Chemical Evolution of Nanostructured Materials by In-Situ Experiments. Microscopy and Microanalysis, 2019, 25, 19-20.	0.2	0